

## Article

# Revolutionizing Urban Pest Management with Sensor Fusion and Precision Fumigation Robotics

Sidharth Jeyabal, Charan Vikram , Prithvi Krishna Chittoor \*  and Mohan Rajesh Elara 

Engineering Product Development Pillar, Singapore University of Technology and Design, Singapore 487372, Singapore; sidharth\_jeyabal@alumni.sutd.edu.sg (S.J.); charan\_vikram@sutd.edu.sg (C.V.); rajeshelara@sutd.edu.sg (M.R.E.)

\* Correspondence: prithvi\_chittoor@sutd.edu.sg

**Abstract:** Effective pest management in urban areas is critically challenged by the rapid proliferation of mosquito breeding sites. Traditional fumigation methods expose human operators to harmful chemicals, posing significant health risks ranging from respiratory problems to long-term chronic conditions. To address these issues, a novel fumigation robot equipped with sensor fusion technology for optimal pest control in urban landscapes is proposed. The proposed robot utilizes light detection and ranging data, depth camera inputs processed through the You Only Look Once version 8 (YOLOv8) algorithm for precise object recognition, and inertial measurement unit data. These technologies allow the robot to accurately identify and localize mosquito breeding hotspots using YOLOv8, achieving a precision of 0.81 and a mean average precision of 0.74. The integration of these advanced sensor technologies allows for detailed and reliable mapping, enhancing the robot's navigation through complex urban terrains and ensuring precise targeting of fumigation efforts. In a test case, the robot demonstrated a 62.5% increase in efficiency by significantly reducing chemical usage through targeted hotspot fumigation. By automating the detection and treatment of breeding sites, the proposed method boosts the efficiency and effectiveness of pest management operations and significantly diminishes the health risks associated with chemical exposure for human workers. This approach, featuring real-time object recognition and dynamic adaptation to environmental changes, represents a substantial advancement in urban pest management, offering a safer and more effective solution to a persistent public health issue.



**Citation:** Jeyabal, S.; Vikram, C.; Chittoor, P.K.; Elara, M.R. Revolutionizing Urban Pest Management with Sensor Fusion and Precision Fumigation Robotics. *Appl. Sci.* **2024**, *14*, 7382. <https://doi.org/10.3390/app14167382>

Academic Editor: Yutaka Ishibashi

Received: 24 July 2024

Revised: 18 August 2024

Accepted: 20 August 2024

Published: 21 August 2024



**Copyright:** © 2024 by the authors. Licensee MDPI, Basel, Switzerland. This article is an open access article distributed under the terms and conditions of the Creative Commons Attribution (CC BY) license (<https://creativecommons.org/licenses/by/4.0/>).

**Keywords:** depth camera; fumigation; LiDAR; robot; sensor fusion; YOLO

## 1. Introduction

Mosquito-borne illnesses are still a significant cause of death worldwide, threatening public health [1]. These insects are carriers of viruses, transmitting illnesses such as dengue, chikungunya, dirofilariasis, malaria, and Zika [2–4]. Due to global warming, temperatures are rising, and heat spikes are occurring more often. Researchers have found that mosquitoes adapting to heat spikes have become more pesticide-resistant [5]. The National Environmental Agency (NEA) of Singapore has declared various types of open and closed drains, discarded containers, clogged gutters, and roadside drainage grates as a few of the mosquitoes' most common breeding sites, as illustrated in Figure 1 [6–8]. As a method of population control, fumigation is typically used alongside other methods, such as mosquito traps and lab-grown mosquitoes, which mate with female mosquitoes and make them infertile [9]. Active and passive traps [10] combat increasing populations of mosquitoes. Active traps use gaseous chemicals such as carbon dioxide (CO<sub>2</sub>) and visual attractants such as light, while passive traps use sticky surfaces to trap mosquitoes. Some examples of traps that have been used and studied are the Biogents sentinel trap, which uses CO<sub>2</sub> [11], light traps [12], ovitraps, which serve as a place for mosquitos to deposit eggs into larvicide, effectively killing the hatched eggs [13], and gravitraps, which function

like ovitraps [14]. However, each of these traps has its limitations. The Biogents Sentinel trap is much more effective when paired with another attractant, such as the BG Lure [15]. Light traps are inefficient when there are high mosquito densities [16]. Ovitrap are not as efficient as other traps, such as the host-seeking female traps [17]. Lastly, gravitraps are not as efficient as suction fan traps and have the limitation of trapping male mosquitoes [18]. Thus, fumigation has proven to be very effective in mosquito population control. Manual fumigation by humans is a laborious task, and there is a chance that humans may overlook specific breeding grounds. According to the NEA, hydrogen cyanide, methyl bromide, and hydrogen phosphide are common fumigants [19]. Overexposure to fumigants can impact the central nervous system [20,21]. Thus, robots can assist in automating mosquito breeding ground detection and fumigation.



**Figure 1.** Common mosquito breeding sites in urban landscapes.

In previous works, researchers have demonstrated an Unmanned Aerial Vehicle (UAV)-based fumigation robot that identifies possible mosquito breeding grounds [22]. However, it is not easy for UAVs to fumigate small areas on the ground as UAVs are better designed for widespread area coverage during spraying, as used in the agriculture industry. Due to the height from which the fumigants are sprayed, there is a chance that the fumigants may not reach the intended mosquito breeding ground. Environmental factors, such as wind, may also blow the fumigants away before they reach the hotspot, deeming it ineffective [23,24]. Ground robots are safer as there is no risk of collisions with birds in the sky or the robot failing mid-air and falling to the ground. Furthermore, a land robot's energy expenditure is better spent on locomotion. Researchers [25] employed deep learning models, specifically various YOLO-based architectures, to identify and target specific areas within tobacco fields for treatment. This approach optimizes the application of agrochemicals, reducing waste and environmental impact, and addresses challenges such as pressure fluctuations during spraying [25–28]. The study developed by [29] presents an electric sprayer with a crop perception system that calculates leaf density using a support vector machine (SVM). This system, tested with a dataset created for the community, achieved an accuracy between 80% and 85%, enhancing spraying accuracy and precision. This emphasizes the effectiveness of integrating machine learning for precise chemical applications. Researchers [30] enhanced a YOLOv5 model for precise plant detection, which significantly improved the accuracy and efficiency of a precision spraying robot. Integrating an attention mechanism and the C3-Ghost-bottleneck module boosted performance, increasing the mean average precision (*mAP*) by 3.2%. The work presented in [31] introduces a robotic weeding system that minimizes herbicide usage through precise application. It featured a stereo camera, an inertial measurement unit, and spray nozzles controlled by a binary linear programming-based algorithm for optimal coverage. A study [32] presented a deep learning-based detection model that distinguished weeds from cotton seedlings with high accuracy by using a convolutional block attention module (CBAM), a Bidirectional Feature Pyramid Network structure (BiFPN), and a bilinear interpolation algorithm.

Existing systems, while advanced, primarily focus on agricultural settings with structured environments and often lack the capability to navigate the complex, dynamic, and GPS-denied environments typical of urban landscapes. A comprehensive review of the ex-

isting literature (Table 1) shows a notable deficit in real-time autonomous dynamic hotspot mapping and fumigating robots. This absence underscores the novelty and importance of the proposed contribution, which introduces an innovative system specifically tailored for urban settings. The proposed fumigation robot aims to fill this gap by utilizing advanced sensor fusion and AI-based detection algorithms [33], ensuring precise and effective pest control in challenging urban terrains. Furthermore, integrating AI-based detection in precision fumigation enhances the robotic system's ability to perform targeted actions effectively. The system ensures that interventions are precise and efficient by leveraging advanced AI algorithms for detection and identification. This approach is particularly beneficial in densely populated urban areas where mosquito control must be meticulously managed to maximize impact while minimizing chemical usage, highlighting the robot's potential to transform urban pest management practices. From the literature survey, the following highlights are identified:

**Table 1.** Comparison table contrasting the existing methods with the proposed work.

Aspect	Existing Methods	Proposed Work
Technology Used	<ul style="list-style-type: none"> <li>Manual fumigation, breeding infertile mosquitoes</li> <li>Biogents sentinel trap, light traps, ovitraps, and gravitraps</li> </ul>	<ul style="list-style-type: none"> <li>Sensor fusion (LiDAR, depth camera with YOLOv8, IMU)</li> <li>3D-LiDAR for mapping and navigation</li> </ul>
Primary Limitations	<ul style="list-style-type: none"> <li>Overexposure to chemicals affecting health</li> <li>Inefficiency in high mosquito densities</li> <li>Limited field of view (2D-LiDAR)</li> </ul>	<ul style="list-style-type: none"> <li>Requires sophisticated technology and initial setup</li> </ul>
Efficiency	Varies significantly with manual fumigation and trap effectiveness	High efficiency due to automated, precise detection and fumigation of hotspots
Health Impact	Potential health risks due to chemical exposure	Reduced risk to human operators by automating chemical fumigation
Environmental Impact	Potential for chemical dispersal affecting non-target areas	Focused application of chemicals, reducing environmental footprint
Navigation and Mapping	Limited in non-open areas like indoor environments or dense urban settings	Advanced navigation using 3D-LiDAR and LIO-SAM algorithm, improving accuracy in complex environments
Hotspot Identification	Relies heavily on manual inspection and stationary traps	Automated real-time identification and remapping, increasing responsiveness to changing conditions
Operational Strategy	Static with periodic manual adjustments	Dynamic, with ongoing adjustments based on real-time data collection
Cost	Lower initial cost but higher due to labor and repeated interventions	Higher initial investment but lower ongoing costs due to automation
Adaptability	Limited adaptability to new breeding grounds without manual intervention	High adaptability with continuous learning and updating capabilities

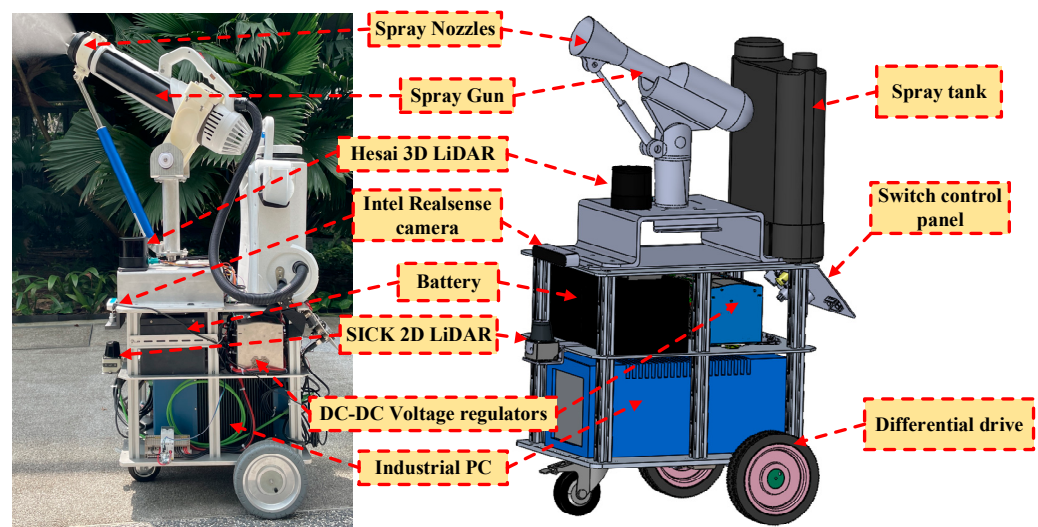
The main contributions of this paper are as follows:

1. The development of a precision fumigation robot for urban landscapes: This is an original contribution, as no existing autonomous robots navigate urban environments for precision fumigation applications. This novel development addresses the need for precise, automated solutions in urban pest control.
2. The development of a LiDAR-Vision-IMU fusion algorithm: Inspired by existing research [34,35], this contribution enhances traditional sensor fusion techniques to fit an autonomous fumigation robot, improving its ability to identify and map mosquito

hotspots in real time. This adaptation enables more effective data collection and targeting of potential breeding hotspots.

## 2. Development of the Fumigation Robot

The fumigation robot shown in Figure 2 is designed to identify and fumigate mosquito hotspots. The robot's motion is based on differential drive, allowing it to maneuver easily during fumigation. The robot uses 2D and 3D LiDARs and an inertial measurement unit for autonomous navigation. The robot is also equipped with a spray gun and a chemical tank. The spray gun's top and bottom ends are connected to one end of the linear actuator. The opposite end of the linear actuator is attached to the bottom end of the metal shaft. The system is on top of a stepper motor to allow for the panning motion of the gun. The linear actuator facilitates the tilt motion of the spray gun. The adjustable gun can rotate 360° and fumigate up to 4.5 m from the ground and 2.5 m to 6 m away from the robot. The specifications of the major components are listed in Table 2.



**Figure 2.** Fumigation robot and its major components.

**Table 2.** Major components of the proposed precision fumigation robot.

Product	Specifications
Oriental motors	BLHM450KC-30
IMU	Vectonav VN-100
Voltage regulator	DDR-480C-24, DDR-240C-24
2D LiDAR	SICK TiM581-2050101
3D LiDAR	Hesai QT128
Depth camera	Intel RealSense D435i
Industrial PC (IPC)	Nuvo-10108GC-RTX3080
Battery	48 V, 25 Ah, Lithium Iron Phosphate
Fogging unit	10 L tank, 50-micron droplet size, and flow rate 330 mL/min

In this paper, mosquito breeding grounds are referred to as hotspots as these are considered the “ground zero” for the growth of the mosquito population. The main aim of the fumigation robot is to identify possible mosquito hotspots and fumigate them. For the robot to work efficiently, daily remapping is necessary so that the robot can locate new hotspots and fumigate them while being able to identify when a hotspot is no longer active and halt fumigation for the area.

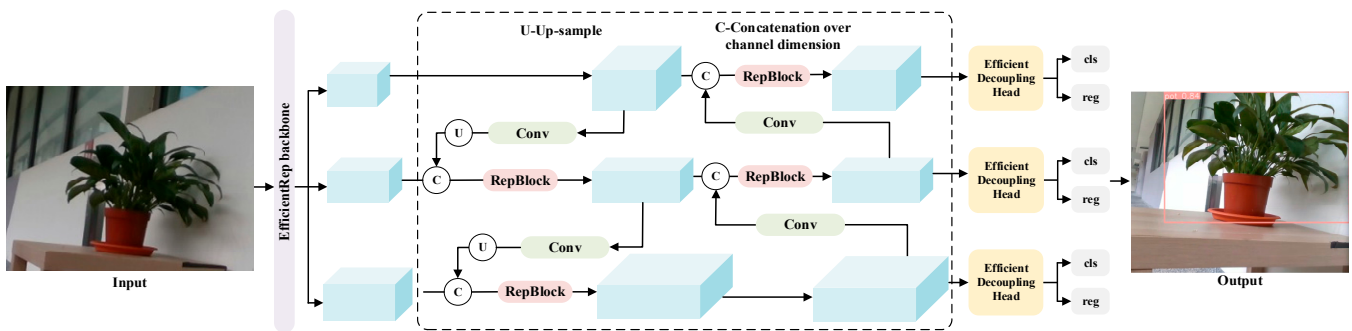
### 2.1. Setting Up the Navigation Stack

In the proposed system, fumigation is performed autonomously around an area, and those hotspots are mapped in real time in the robot's map database. For autonomous navigation, there are different levels of execution. The first step is the mapping of the environment. Various sensors for mapping the environment are depth cameras, 3D Light Detection and Ranging (LiDAR), and 2D-LiDAR. In this research, a 3D-LiDAR is used instead of other sensors to map the environment. Three-dimensional-LiDAR is better for mapping than the passive mapping method using depth cameras [36]. Moreover, depth cameras are affected by illumination, and many details are lost depending on how well-lit the environment is. Two-dimensional-LiDARs have a very limited field of view, as any object below or above its scan area is undetected. Hence, considering all these points, a 3D-LiDAR is used for this application. There are different mapping algorithms used in most 3D-LiDAR integrated systems, namely Lidar Odometry and Mapping (LOAM), Cartographer by Google, High-Definition LiDAR (HDL) graph simultaneous localization and mapping (SLAM), and Lidar Inertial Odometry via Smoothing and Mapping (LIO-SAM). Compared to the existing mapping algorithms, LOAM was the best until a few years ago. It was even the top-ranked LiDAR-based method in the Karlsruhe Institute of Technology and Toyota Technological Institute (KITTI) dataset benchmark site. However, drifting in large-scale tests came with a significant drawback. Hence, LIO-SAM [37] is used contrary to the LOAM in the proposed system. In the experimental results, the LIO-SAM showed a translation error of 0.96 compared to LOAM, which had a translation error of 47.31%. Following the creation of the detailed map, navigation must be carried out. The navigation history goes back to the Devish robot, designed to carry out navigation inside office ecosystems [38]. These navigation stacks used finite state machine (FSM) for less complex environments; hence, a behavior tree was used inside navigation stacks to make decisions on complex tasks. For example, in [39], shooting tactics in soccer games were decided using a decision tree, which would never have been possible with FSM. These decision trees are used in navigation. The navigation stack by the robot operating system (ROS) is the most widely used, and its successor is Navigation2. It was built for ROS2, which uses Data Distribution Service (DDS) for communication. DDS is an industrial communication protocol that offers secure data transmission between robots. Navigation2 stack has been released for different motions of robots, namely differential, holonomic, legged, and Ackermann, for a wide spectrum of environments. In the proposed system, the Navigation2 stack is used for navigation.

### 2.2. Training Hotspots Using YOLOv8

Any autonomous robot that navigates must perceive the environment and obtain details to act accordingly. To serve this purpose, there are different detection algorithms, such as Faster Region-based Convolutional Neural Network (Faster R-CNN) [40], Faster R-CNN VGG-16 [41], faster deformable part model (Fastest DPM) [42], and YOLO [43]. In [43], experimental results on the visual object classes dataset showed that Fast-YOLO, one of the successors of the well-performing model YOLO, was able to perform better with an *mAP* score of 63.4% and 155 frames per second, which was, on average, two times faster than other detection models. There have been many versions of YOLO, and for the proposed system, the YOLOv8 algorithm was used, and it proved to be faster and lighter than its predecessors. The detected objects using YOLOv8 are put inside the map to identify the fumigation hotspots. The YOLOv8 is a cutting-edge object detection model known for its exceptional speed and accuracy, making it ideal for real-time applications. Building on the strengths of its predecessors, YOLOv8 introduces advanced features, such as anchor-free detection, which simplifies the model and enhances its generalization capabilities. It leverages the latest advancements in deep learning architectures, including Cross-Stage Partial (CSP) connections and Path Aggregation Network (PAN), for superior feature extraction and aggregation.

The architecture of YOLOv8, as shown in Figure 3, is designed for efficient and precise object detection, comprising a backbone, neck, and head. The backbone incorporates EfficientRep blocks inspired by MobileNet and EfficientNet, utilizing depthwise separable convolutions and squeeze-and-excitation modules to optimize performance. It also includes Reparameterized VGG block (RepVGG) blocks, simplifying complex structures for improved inference efficiency. The neck features convolutional blocks enhanced with activation functions like leaky rectified linear unit, which introduce non-linearity and assist in primary feature extraction. RepBlocks, configured differently for training and inference, facilitate better learning while reducing computational load. The upsampling layers increase the spatial dimensions of the feature maps, which is crucial for detecting smaller objects.



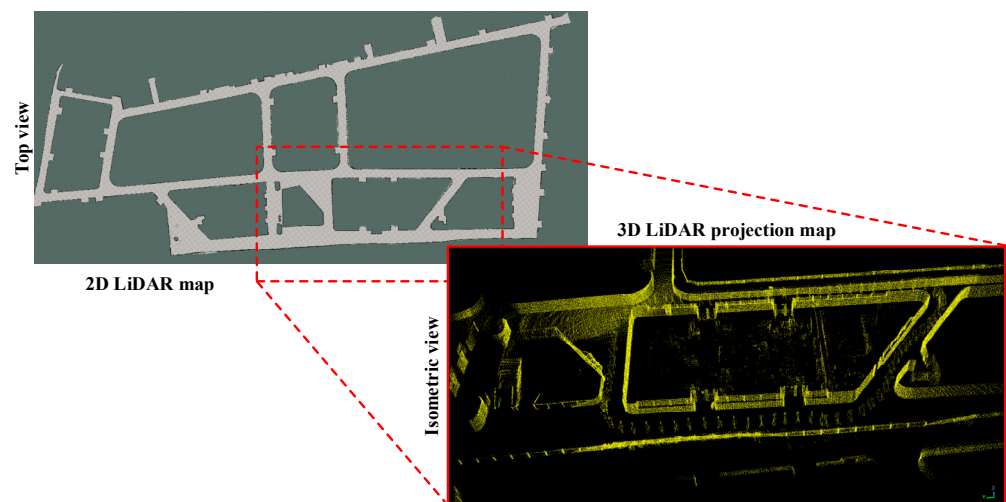
**Figure 3.** YOLOv8 architecture for detecting hotspots.

The head of YOLOv8 features an Efficient Decoupled Head, which separates classification and localization tasks into distinct branches, leading to more accurate detections. This architecture ensures that the model identifies and classifies objects, making it a powerful tool for real-time detection applications. A database keeps track of the fumigation locations. The robot uses this information to generate a prioritized sequence order to navigate from one point to another and fumigate in the shortest time. All the operations on the robot side that perform navigation and fumigation are controlled using ROS. As the robot is deployed in semi-outdoor and outdoor scenarios, SLAM algorithms like High-Definition LiDAR (HDL) graph slam map the environment and later localized using HDL localization for precise accuracy.

### 3. Mapping and Hotspot Identification

#### 3.1. Autonomous Exploration of the Robot

The fumigation robot developed aims to find mosquito hotspots. In the proposed approach, the robot explores the environment, identifies the hotspots, and saves the position of those hotspots. Before identifying hotspots, a map of the environment is needed for the robot to navigate through it. The proposed system opted for an occupancy grid-based 2D map. Different occupancy grid mapping techniques exist, such as hector slams, gmapping, and cartography. The map produced consists of cells. Each cell has cost values associated with it, signifying the presence and absence of the object. If the object is present, then a high-cost value is given to the cell. Usually, black spots are considered obstacles, and grey areas are considered accessible areas, as shown in Figure 4. The occupancy grid map was made using a SICK TIM351 LiDAR. The ROS package used for this was gmapping. This package takes in laser-scan data from the sick\_tim package and converts the data into an occupancy grid map. The map of the environment generated from the 2D and 3D LiDARs is illustrated in Figure 4.



**Figure 4.** Comparative maps of the test environment using 2D and 3D LiDAR scans. The 2D scan provides a flat, top-down view, while the 3D scan offers a detailed, multi-dimensional representation, capturing height and depth for enhanced spatial awareness and navigation.

### 3.2. Hotspot Identification Training

The main objective of the robot is to find the hotspot using an object detection model. Detection models like Faster R-CNN, ResNet, RetinaNetV2, and YOLO series detection models exist. YOLO has been used for research, specifically YOLOv8, because the YOLO series of object detection models perform well for videos, and YOLOv8 being computationally light makes it the first choice for our purpose. A comparative analysis of YOLOv8 was carried out with YOLOv2, YOLOv3, YOLOv4, and YOLOv5 versions in [44]. According to [45], YOLOv8 is the same as YOLOv5, with some minor differences between them:

- The C3 module is replaced with the C2f module,
- YOLOv5 does not have convolution layers 10 and 14,
- The bottleneck layer was tampered, where  $1 \times 1$  layer was replaced with  $3 \times 3$  convolution layers and the decoupled head was used instead of the objectness step [44].

YOLOv8 introduces several improvements over YOLOv5, enhancing its effectiveness in object-detection tasks. Replacing the C3 module with the C2f module enhances feature-processing capabilities, which increases accuracy. Removing specific convolution layers leads to a more streamlined architecture, reducing computational demands. Changes in the bottleneck layer, such as replacing  $1 \times 1$  with  $3 \times 3$  convolution layers, allow for better feature capture. Additionally, using a decoupled head instead of the objectness step improves the precision of both localization and classification tasks, making YOLOv8 a robust option for real-time applications. Table 3 illustrates the details of the IPC used for training. YOLOv8 performed comparatively better with a lesser number of datasets and computational requirements. Compared to its previous counterparts, this model is different. YOLOv8 is an anchor-free model, accounting for lower bounding box predictions that result in faster Non-Maximum Suppression. YOLOv8 was trained on different hotspots, namely dustbins, coolers, drains, plants, pots, buckets, and toilets [46]. In total, 5000 images were annotated to create a diverse dataset. Image-level data augmentation, such as shear, rotation, cut-out, and noise, was carried out before training, with the training and validation images split in an 80:20 ratio.

**Table 3.** Detailed specifications of the IPC used for training the hotspot dataset.

Component	Detailed Specification
CPU	Intel i7 12th-Gen Core 65 W LGA1700 CPU
RAM	64 GB DDR5 4800 MHz
Graphics	NVIDIA RTX 4080 16 GB
SSD	NVMe SSD 2 TB Gen4 M.2 2280
Temperature	Rugged, $-25\text{ }^{\circ}\text{C}$ to $60\text{ }^{\circ}\text{C}$ operation
DC Input	3-pin + 4-pin pluggable terminal block for 8 V to 48 V DC input with ignition control, Humidity: 10~90%, non-condensing
Vibration and Shock absorption	MIL-STD-810H, Method 514.8, Category 4 (with damping bracket)

### 3.3. Dynamic Map Update

The generated map has a lot of obstacles, and robots must avoid them during the exploration. While doing so, the robot looks for hotspots for fumigation. In addition to saving the hotspot location, it is displayed as a marker inside the map in real time. Transformation plays a major role in updating the map. It is a concept through which points in one frame can be converted with respect to another frame. Here, all the objects detected are published with respect to the camera frame. However, to put those objects inside the map, it must be published with respect to the map frame.

The system has two nodes running in parallel; one node called Detection.py, with its pseudocode presented in Algorithm 1, is responsible for detecting the objects and converting the location obtained into the map frame, then another node called Marker.py converts the object's location into a visualization marker. The Detection.py node, apart from localizing objects, also scores the object; thus, during multiple instances, if the same object is detected, the object's location is provided with a score signifying the importance of the hotspot. The overall workings of the proposed system are shown in Figures 5 and 6.

---

#### Algorithm 1: Detection.py

---

##### Initialize parameters and variables

Define read\_csv function

Define write\_csv function

##### Main program execution:

Start RealSense pipeline

Initialize ROS node and publishers

Initialize variables for pose tracking and detection

Start main loop:

Obtain color and depth frames

Detect objects in color frame using YOLO

##### Iterate over detected results:

Extract bounding box coordinates

Calculate object center

Estimate object depth

Transform object pose to map frame

Read existing data from CSV

##### Compare current pose with existing entries:

If match found:

Update score for object

If no match found:

Append new entry with object's pose and prev\_score

Write updated data back to CSV

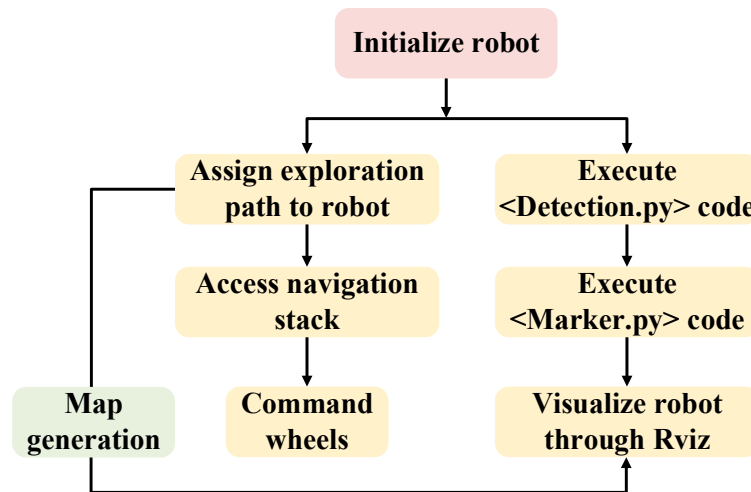
Visualize detected objects and scores on color image

Display color image with annotations

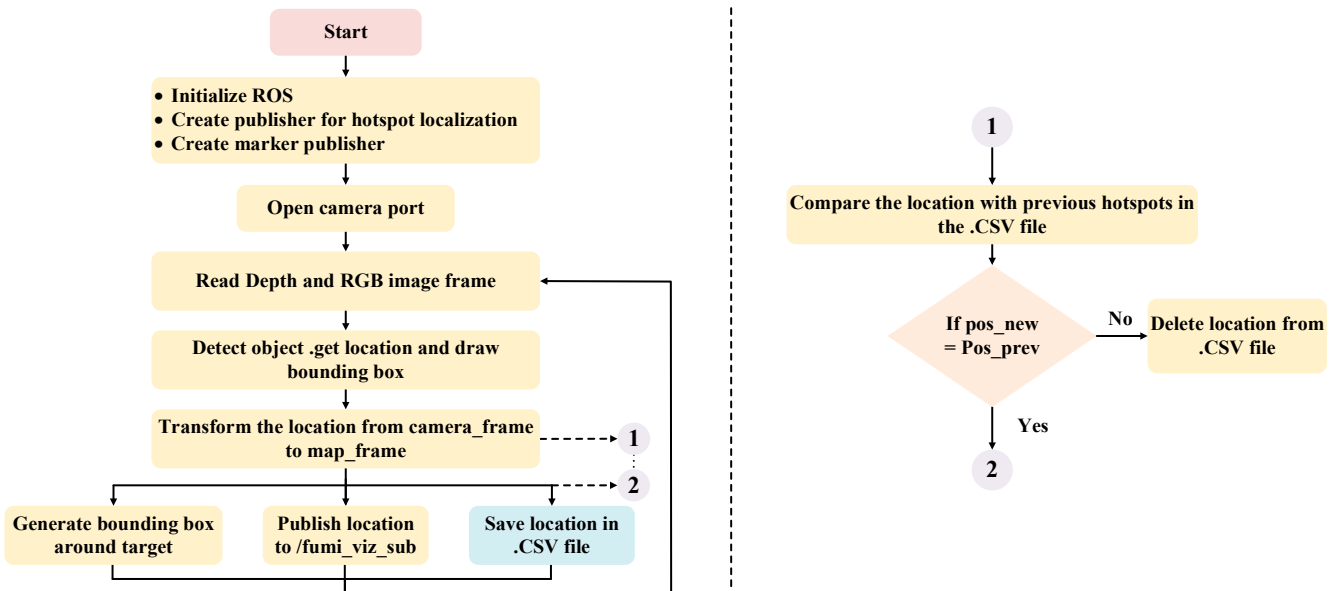
Wait for user input to exit program

---





**Figure 5.** Overview of the proposed system’s workflow, from robot initialization and path assignment to executing detection and marker scripts, navigation control, map generation, and robot visualization via RViz.



**Figure 6.** Flowchart illustrating the process of hotspot identification and dynamic updating over time. The system initializes, captures image data, detects and localizes hotspots, and updates the map by comparing new and previous locations, ensuring accurate and current hotspot mapping for targeted interventions.

Figures 7 and 8 outline the process where the fumigation robot updates hotspot markers in real time by detecting potential mosquito breeding hotspots and recording their positions. Initially, the robot opens the test location map and initializes its sensors, including a 2D LiDAR, 3D LiDAR, and depth camera. These sensors scan the environment to identify potential hotspots and help avoid obstacles that are hard to detect [47]. The identified hotspots are then marked on the map. The robot employs the YOLOv8 algorithm to detect specific objects within these hotspots, extracting their  $x$  and  $y$  coordinates. LiDAR data are used to determine the  $z$  coordinate, creating a complete 3D localization of the detected objects. This information is used to update the map with the precise locations of the hotspots. The markers for these hotspots are then overlaid on the real-time map, with a weight assigned to each  $x$ ,  $y$ , and  $z$  position to indicate whether it is a temporary

or permanent hotspot. This system allows for dynamic 3D visualization and recording of hotspot areas, enhancing the robot’s ability to target fumigation efforts effectively.

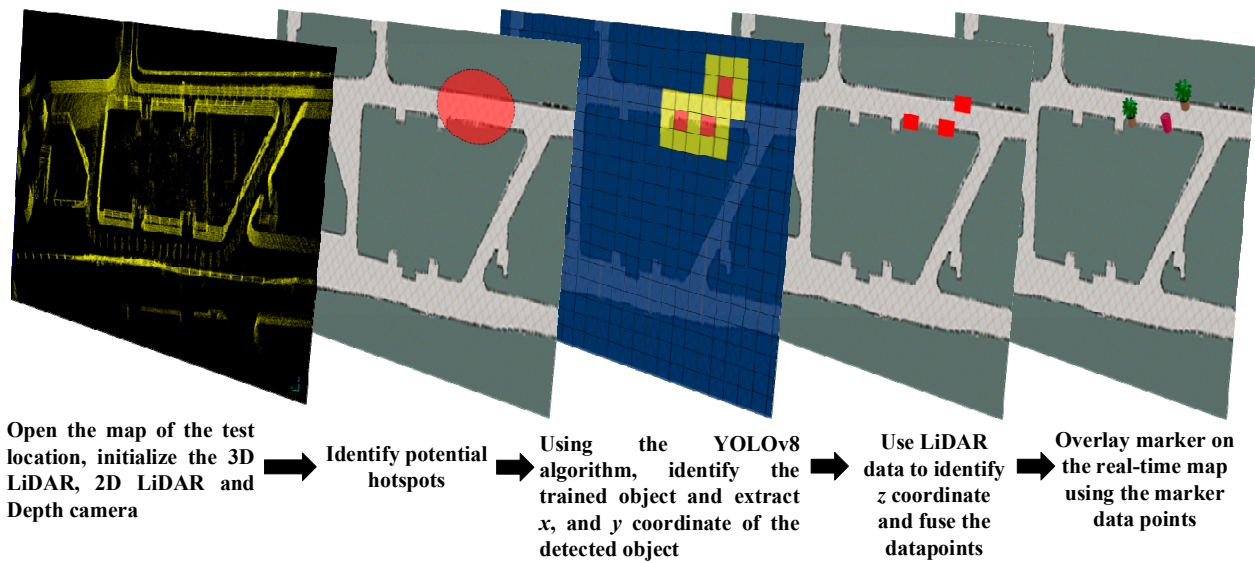


Figure 7. The process flow of updating hotspot markers on the real-time map.

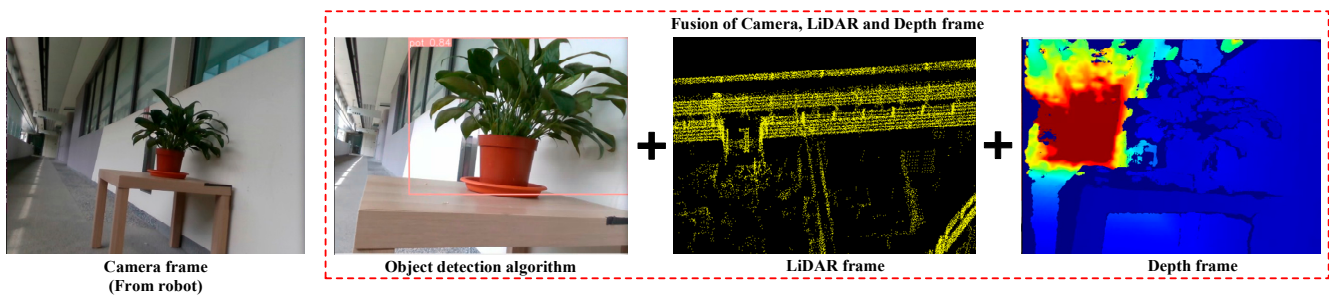


Figure 8. Fusion of YOLOv8, LiDAR frame, and depth camera frame for precision identification and localization of fumigation hotspot.

#### 4. Results and Discussion

##### 4.1. Performance Metric Analysis

The YOLOv8 detection model is trained for five hotspots: dustbin, cooler, drain, toilet, and pot. The performance analysis of the detection model was carried out using the most trusted parameters, such as  $F_1$  score,  $mAP$ ,  $recall$ , and  $precision$ . A high  $F_1$  score means the detection model balances  $recall$  and  $precision$  well;  $mAP$  provides a comprehensive performance analysis across various classes and localization accuracies.  $Recall$  is the measure of detecting objects even at the risk of false positives, and  $precision$  focuses on the model’s objective to avoid false positives. Each of the parameters is calculated based on false positives ( $fp$ ), false negatives ( $fn$ ), true negatives ( $tn$ ), and true positives ( $tp$ ). The formulae for each parameter are given below.

$$Precision (P) = \frac{t_p}{t_p + f_p} \tag{1}$$

$$Recall (R) = \frac{t_p}{t_p + f_n} \tag{2}$$

$$F_{measure}(F_1) = \frac{2 \times precision \times recall}{precision + recall} \tag{3}$$

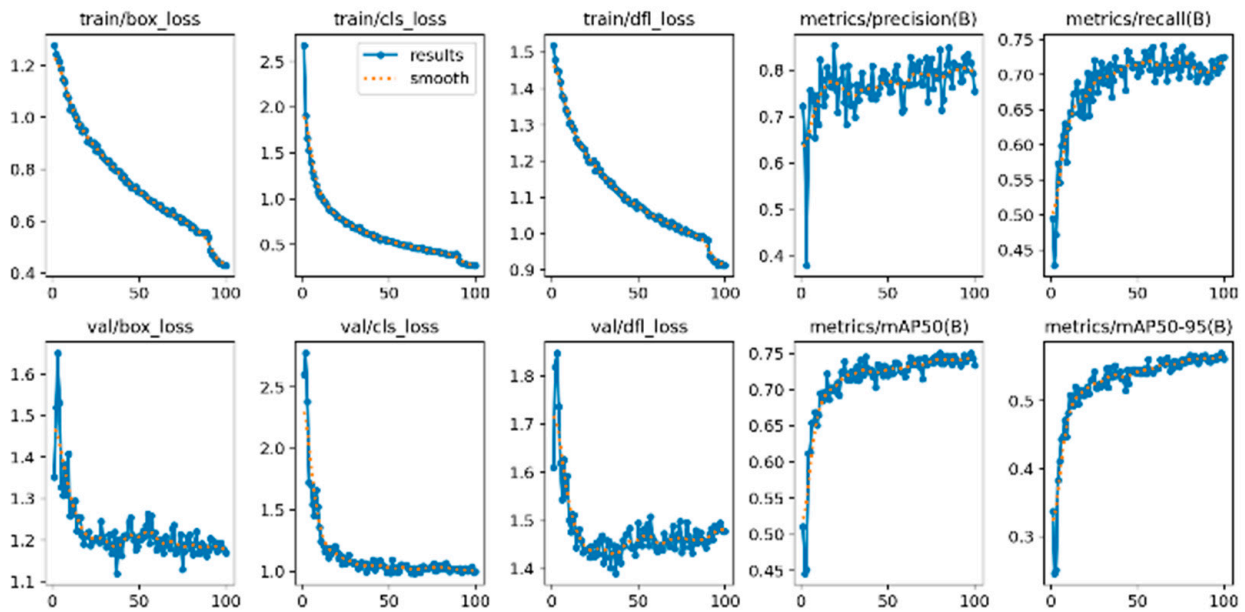
$$mAP = \frac{1}{n} \sum_{i=1}^n AP_i \tag{4}$$

It can be seen in Table 4 that the model trained has a high precision value of 0.81, which means there are fewer chances of false positives. Since the proposed work is not strict in identifying the nature of the hotspot, a slightly low recall value is good enough, which is evident from the  $F_1$  score. The detection for this current research was conducted on dustbins and pots. Though the dustbin has a  $mAP$  value lower than that of other classes, it gave us a fair performance during our experiment.

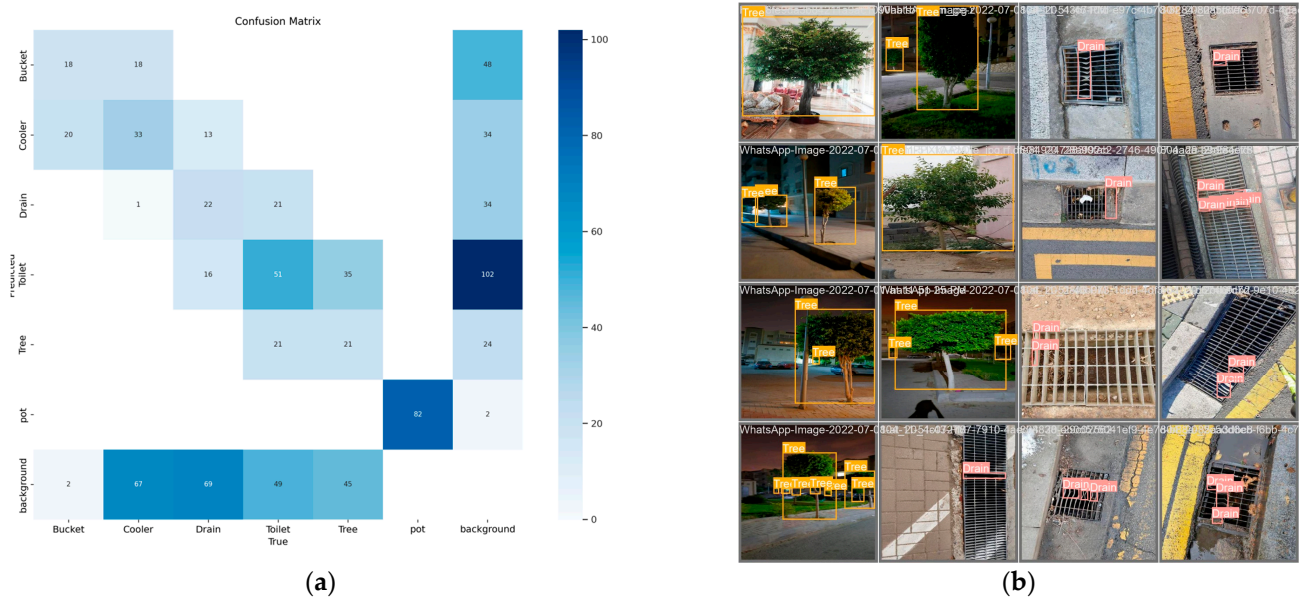
**Table 4.** Performance metrics of the YOLOv8 detection model used in the proposed precision fumigation robot.

Type	Precision	Recall	$F_1$ Score	mAP@0.5 (%)
All	0.81	0.69	0.74	0.74
Cooler	0.82	0.84	0.83	0.93
Drain	0.95	0.91	0.93	0.94
Toilet	0.87	0.88	0.88	0.94
Dustbin	0.75	0.51	0.61	0.62
Pot	0.99	1	0.99	0.99

A performance comparison test was performed to check the effectiveness of the proposed model compared to other detection models. The proposed system is more particular about the model’s input as video; thus, the other models are eliminated, and a performance evaluation test is performed among the YOLO series of models. Each of these models was trained with the same number of datasets. Figure 9 shows the overall result of the trained model. Figure 10 shows the confusion matrix and detection results from the YOLOv8.



**Figure 9.** Training and validation metrics for YOLOv8, showing the progression of losses (box, classification, and objectness) and performance metrics ( $precision$ ,  $recall$ ,  $mAP@0.5$ , and  $mAP@0.5:0.95$ ) over 100 epochs. The graphs illustrate the model’s improvement in accuracy and reduction in errors as training progresses, with consistent convergence observed in both training and validation phases.



**Figure 10.** (a) Confusion matrix for YOLOv8 on the given dataset, illustrating the model's performance across different classes such as cooler, drain, toilet, dustbin, and pot. (b) Object detection results using YOLOv8, identifying trees and drains in various urban environments. The model successfully detects and labels these objects across different lighting conditions and angles, demonstrating its robustness and accuracy in real-world scenarios.

YOLOv8 achieves a *Precision* of 0.81, a *Recall* of 0.71,  $F_1$  score of 0.75, and a *mAP* of 0.74, outperforming the other models across all metrics. Specifically, compared to Faster RCNN ( $P$ : 0.564,  $R$ : 0.61,  $F_1$ : 0.58, *mAP*: 0.57), YOLOv8 shows a 43.7% improvement in *Precision*, a 15% increase in *Recall*, a 27.3% boost in  $F_1$  score, and a 29.8% enhancement in *mAP*. When compared to YOLOv5 ( $P$ : 0.73,  $R$ : 0.60,  $F_1$ : 0.65, *mAP*: 0.69), YOLOv8 demonstrates an 11% improvement in *Precision*, an 18.3% increase in *Recall*, a 15.4% boost in  $F_1$  score, and a 7.2% enhancement in *mAP*. Similarly, compared to YOLOv7 ( $P$ : 0.70,  $R$ : 0.58,  $F_1$ : 0.63, *mAP*: 0.61), YOLOv8 shows a 15.7% improvement in *Precision*, a 22.4% increase in *Recall*, a 19% boost in  $F_1$  score, and a 21.3% enhancement in *mAP*. These quantitative improvements indicate that YOLOv8 is more reliable, offering higher precision and recall rates, translating to fewer *fp* and *fn*. The efficiency gains in terms of  $F_1$  score and *mAP* also suggest that YOLOv8 provides a more balanced and accurate detection.

It can be inferred from Table 5 that the selected YOLO model has good precision compared to other models, which means it is the best at avoiding *fp*. The *mAP* score (0.74) for YOLOv8 is better than that of the other models, which means it is better at localizing objects. Considering the above points, YOLOv8 was chosen as the object detection model.

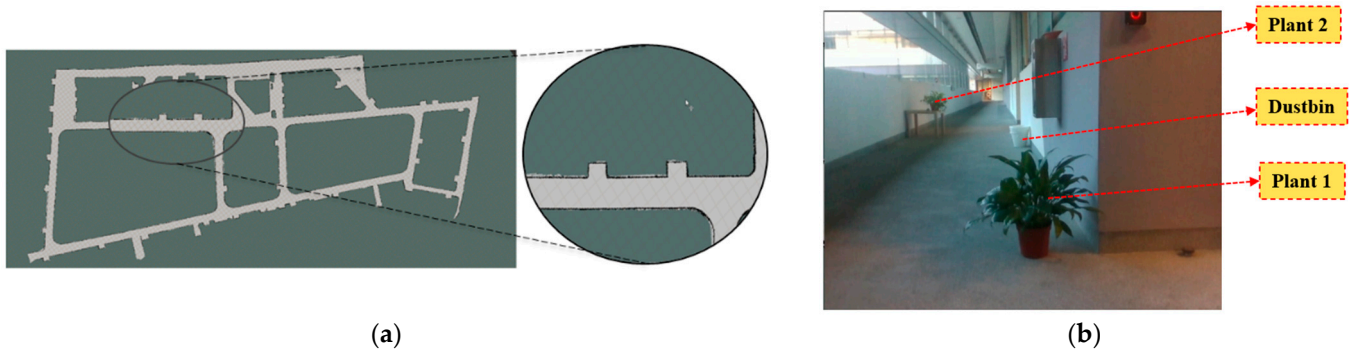
**Table 5.** Performance comparison with different YOLO versions and faster RCNN detection models for the dataset used in training the mosquito hotspots.

Model	Precision ( $P$ )	Recall ( $R$ )	$F_1$ Score ( $F_1$ )	<i>mAP</i> @0.5 (%)
Faster RCNN	0.56	0.61	0.58	0.57
YOLOv5	0.73	0.60	0.65	0.69
YOLOv7	0.70	0.58	0.63	0.61
YOLOv8 (current model)	0.81	0.71	0.75	0.74

#### 4.2. Test Site Description

The site chosen for the experiment is a pathway in Level 6 of Building 2 at the Singapore University of Technology and Design. The pathway is well-lit with natural light. A small

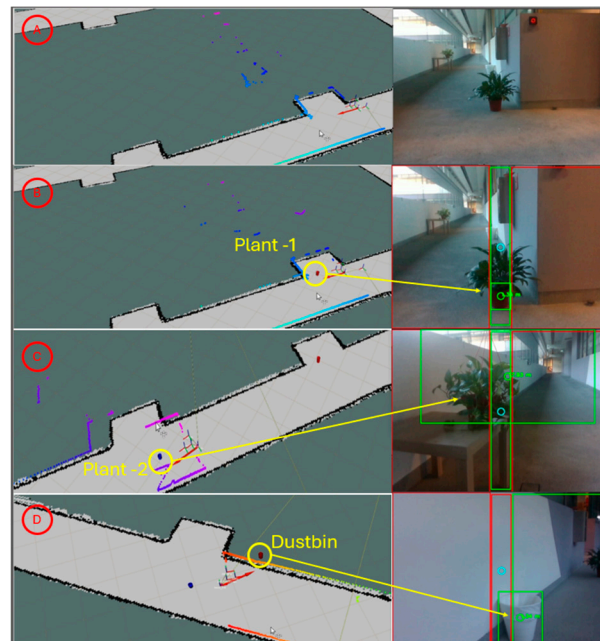
portion of the building was taken for experimentation, as shown in Figure 11. The objects identified along the pathway were dustbins and pots.



**Figure 11.** (a) Two-dimensional map of the test site and (b) the placement of trained objects for the robot to detect potential hotspots.

#### 4.3. Hotspots Identification and Plotting on the Map

The potential breeding grounds for mosquitoes were identified during the robot’s exploration phase. As depicted in Figure 12, the robot navigates through the environment, utilizing its sensors to detect and mark hotspots on the map. During its traversal, the robot leverages its integrated LiDAR, depth camera, and YOLOv8 algorithm to precisely identify locations that are likely to serve as breeding grounds for mosquitoes. In this particular scenario, the chosen hotspots include plants and dustbins.



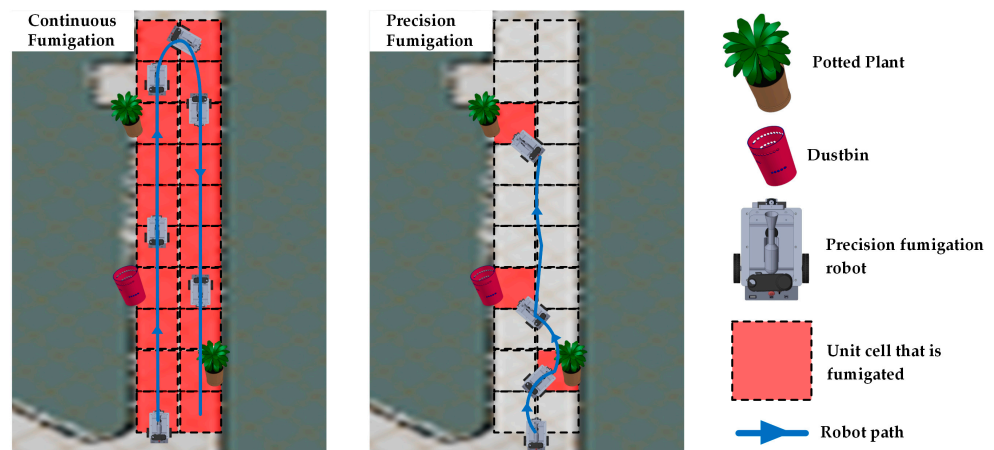
**Figure 12.** Sequential updates of the hotspot map during the robot’s exploration. In panel (A), no hotspots are detected. Panel (B) shows the detection and mapping of “Plant-1”, marked on the map and visually confirmed in the environment. Panel (C) adds “Plant-2” to the map, illustrating the robot’s ability to identify and log new hotspots continuously. Finally, panel (D) shows the detection of a “Dustbin”, further updating the map. Each detected hotspot is localized in the mapped environment and the corresponding real-world image, demonstrating the system’s effectiveness in real-time hotspot identification and mapping.

A comparative analysis (Table 6) of chemical usage in two fumigation scenarios using a precision fumigation robot was conducted, as illustrated in Figure 13. The robot, equipped

with a 10 L capacity spray gun discharging at 330 mL per minute, was tested over a  $10\text{ m} \times 2\text{ m}$  area divided into  $1\text{ m}^2$  unit cells. The first scenario involved continuous fumigation of the entire area, with the robot moving at a speed of 0.5 m/s. The total time required to fumigate the  $20\text{ m}^2$  was 40 s, resulting in a chemical usage of 220 mL. In the second scenario, the robot discreetly fumigated identified hotspots within the same area. Three hotspots were identified, with each being sprayed for 5 s. The total time spent fumigating these hotspots was 15 s, leading to a chemical usage of 82.5 mL. The comparison demonstrates that precision hotspot fumigation significantly reduces chemical usage, achieving a savings of approximately 62.5% compared to continuous fumigation. This efficiency is due to the targeted application of the fumigant, conserving resources, and minimizing environmental impact.

**Table 6.** Comparative analysis of continuous fumigation versus precision fumigation using a precision fumigation robot. The table highlights key differences in area coverage, fumigation time, chemical usage, environmental impact, and overall efficiency.

Aspect	Continuous Fumigation	Precision Fumigation
Area Covered	Entire area ( $20\text{ m}^2$ )	Identified hotspots (3 hotspots)
Robot Speed	0.5 m/s	0.5 m/s
Fumigation Time per $\text{m}^2$	2 s	5 s per hotspot
Total Fumigation Time	40 s	15 s
Chemical Usage Rate	330 mL/min	330 mL/min
Total Chemical Used	220 ml	82.5 ml
Chemical Savings	N/A	62.5% (137.5 mL less than continuous)
Environmental Impact	Higher due to full area coverage	Lower due to targeted application
Efficiency	Lower, as it treats the entire area	Higher, with focused treatment of hotspots



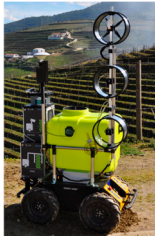

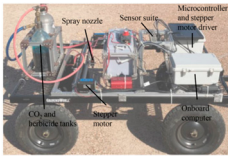


**Figure 13.** Comparison between continuous fumigation (left) and precision fumigation (right) using a precision fumigation robot. The continuous fumigation approach covers the entire area indiscriminately, whereas the precision fumigation approach targets specific hotspots identified within the area, such as potted plants and dustbins. The blue path indicates the robot's movement, while the red-shaded areas represent the regions being fumigated.

#### 4.4. Comparison of Existing Robots with the Proposed Robot

A comparison between the fumigation operation of existing precision spray robots and the proposed precision fumigation robot is illustrated in Table 7. Most precision fumigation robots developed [29–32] so far are tailored for agricultural settings, focusing on optimizing pesticide application in controlled crop environments. These systems, such as those utilizing YOLOv5 and other AI techniques, excel in targeted spraying but lack the adaptability for complex urban landscapes. They are not designed to navigate dynamic urban environments, where the challenges of real-time mapping, precise hotspot detection,

and autonomous navigation are significantly different. The proposed fumigation robot addresses this gap by integrating advanced sensor fusion and YOLOv8 for dynamic hotspot localization, designed explicitly for urban pest control. It offers precise real-time mapping, sophisticated spatial analysis, and adaptability to the complexities of urban navigation, making it a crucial innovation for effective mosquito management in urban settings.

**Table 7.** Comparison between the fumigation operation of existing precision spray robots and proposed precision fumigation robot.

Aspect	Ref. [29]	Ref. [30]	Ref. [31]	Ref. [32]	Proposed Robot
Robot developed					
AI Integration	SVM classifier for leaf density	Improved YOLOv5 model with attention mechanisms	Novel scene representation and motion planning	Deep learning model with CBAM and BiFPN	YOLOv8 for dynamic hotspot localization
Urban Navigation (Complex Environment)	No (focused on agricultural fields)	No (focused on agricultural fields)	No (designed for early-stage crops)	No (agricultural fields only)	Yes (specifically designed for urban landscapes)
Real-Time Operation	Yes, but limited to agricultural fields	Yes, real-time performance with 30 ms/frame detection speed	Yes, sub-centimeter precision in spraying	Yes, real-time detection and spraying	Yes, with real-time mapping and fumigation
Mapping Capabilities	No	No	Limited	No	Dynamic mapping
Precision Targeting	High precision in spraying based on leaf density	High precision for corn and weed identification	High precision for micro-volume spraying	High precision	High precision for mosquito hotspots

#### 4.5. Challenges, Possible Solutions, and Future Research Directions

Many challenges were faced during the development of the robot and the detection algorithm. Some of these challenges can be taken up as future research directions. A few of the challenges and their potential solutions are as follows:

- **Navigation in complex environments:** The differential drive robot is built for navigating in urban environments, where the surface is even and spacious for robot movements. Tracked platforms are effective in handling multiple terrains. However, these platforms consume more energy because they are heavy and bulky, requiring frequent recharging. A modular robot is another future research direction that enables it to change its locomotion system according to the environment.
- **Battery life is a major limitation** restricting the robot’s operational time, necessitating frequent recharging. One possible solution is to have frequent, preferably wireless charging stations that allow full autonomy.
- **Renewable energy sources for charging robots:** Researching the use of renewable energy sources, such as solar power, to extend the operational time of robots and reduce their environmental impact, designing more energy-efficient robots to improve their operational longevity and reduce the need for frequent recharging.
- **Varied environments:** Different environments may require different fumigation strategies, such as discrete fumigating motion, continuous fumigation motion, and 360°

fumigating motion. Using advanced machine learning techniques and identifying the environment, a decision can be made to opt for the required strategy.

- Navigating multiple floors in a building: The proposed challenge can be solved by integrating the robot's control with the building's management system, such as access to calling lifts and doors. However, this requires planning from the initial stage to make the building's infrastructure robot-friendly.

#### 4.6. Limitations

The limitations of the proposed work with the integration of YOLOv8 in the precision fumigation robot are as follows:

- The trained model may underperform in scenarios significantly different from its training environment, restricting its effectiveness in unfamiliar urban landscapes.
- YOLOv8 needs robust computational resources, which could limit the deployment of the robot in settings with limited processing capabilities.
- Optimizing for real-time performance compromises the detection accuracy, which is critical for precise localization of mosquito breeding sites.
- The model's effectiveness decreases with smaller objects, which could be crucial in identifying less conspicuous breeding grounds.
- Vibrations during locomotion affect detection accuracy, leading to blurred images being sent for object recognition.

## 5. Conclusions

The development of a fumigation robot utilizing LiDAR data, depth camera data with YOLOv8 for object recognition, and IMU data represents a significant advancement in targeting mosquito breeding hotspots. Fusing these sensor inputs enables precise localization and comprehensive data collection, ensuring that potential breeding sites are accurately identified and treated. This technology enhances the efficiency of fumigation efforts and significantly reduces human exposure to harmful chemicals, thereby improving safety and operational outcomes. Integrating advanced sensors and algorithms within this robotic system marks a critical step forward in urban pest management, offering a robust solution to a pervasive public health challenge. Further research and development can optimize these systems, making them more adaptable to diverse environments and improving their efficacy in real-world applications.

**Author Contributions:** Conceptualization, S.J. and P.K.C.; methodology, S.J. and P.K.C.; software, S.J. and C.V.; Writing, S.J., C.V. and P.K.C.; resources, M.R.E.; supervision, M.R.E.; project administration, M.R.E.; funding acquisition M.R.E. All authors have read and agreed to the published version of the manuscript.

**Funding:** This research is supported by the National Robotics Programme under its National Robotics Programme (NRP) BAU, Ermine III: Deployable Reconfigurable Robots, Award No. M22NBK0054 and also supported by SUTD Growth Plan (SGP) Grant, Grant Ref. No. PIE-SGP-DZ-2023-01.

**Institutional Review Board Statement:** Not applicable.

**Informed Consent Statement:** Not applicable.

**Data Availability Statement:** The original contributions presented in the study are included in the article, further inquiries can be directed to the corresponding author.

**Conflicts of Interest:** The authors declare no conflicts of interest.

## References

1. Dahmana, H.; Mediannikov, O. Mosquito-borne diseases emergence/resurgence and how to effectively control it biologically. *Pathogens* **2020**, *9*, 310. [[CrossRef](#)] [[PubMed](#)]
2. Franklino, L.H.; Jones, K.E.; Redding, D.W.; Abubakar, I. The effect of global change on mosquito-borne disease. *Lancet Infect. Dis.* **2019**, *19*, e302–e312. [[CrossRef](#)] [[PubMed](#)]



3. Huang, Y.; Higgs, S.; Vanlandingham, D. Arbovirus-mosquito vector-host interactions and the impact on transmission and disease pathogenesis of arboviruses. *Front Microbiol.* **2019**, *10*, 22. [CrossRef] [PubMed]
4. Nguyen-Tien, T.; Lundkvist, Å.; Lindahl, J. Urban transmission of mosquito-borne flaviviruses—a review of the risk for humans in Vietnam. *Infect. Ecol. Epidemiol.* **2019**, *9*, 1660129. [CrossRef] [PubMed]
5. Meng, S.; Delnat, V.; Stoks, R. Mosquito larvae that survive a heat spike are less sensitive to subsequent exposure to the pesticide chlorpyrifos. *Environ. Pollut.* **2020**, *265*, 114824. [CrossRef] [PubMed]
6. Singapore Government. National Environment Agency. Available online: <https://www.nea.gov.sg/> (accessed on 2 January 2022).
7. Dom, N.C.; Ahmad, A.H.; Ismail, R. Habitat characterization of *Aedes* sp. breeding in urban hotspot area. *Procedia-Soc. Behav. Sci.* **2013**, *85*, 100–109. [CrossRef]
8. Wilke, A.B.; Vasquez, C.; Carvajal, A.; Moreno, M.; Fuller, D.O.; Cardenas, G.; Petrie, W.D.; Beier, J.C. Urbanization favors the proliferation of *Aedes aegypti* and *Culex quinquefasciatus* in urban areas of Miami-Dade County, Florida. *Sci. Rep.* **2021**, *11*, 22989. [CrossRef]
9. Liew, C.; Soh, L.T.; Chen, I.; Ng, L.C. Public sentiments towards the use of Wolbachia-*Aedes* technology in Singapore. *BMC Public Health* **2021**, *21*, 1417. [CrossRef]
10. Ahmed, T.; Hyder, M.Z.; Liaqat, I.; Scholz, M. Climatic conditions: Conventional and nanotechnology-based methods for the control of mosquito vectors causing human health issues. *Int. J. Environ. Res. Public Health* **2019**, *16*, 3165. [CrossRef] [PubMed]
11. Wilke, A.B.; Vasquez, C.; Carvajal, A.; Moreno, M.; Petrie, W.D.; Beier, J.C. Evaluation of the effectiveness of BG-Sentinel and CDC light traps in assessing the abundance, richness, and community composition of mosquitoes in rural and natural areas. *Parasites Vectors* **2022**, *15*, 51. [CrossRef] [PubMed]
12. Jhaiaun, P.; Panthawong, A.; Saeung, M.; Sumarnrote, A.; Kongmee, M.; Ngoen-Klan, R.; Chareonviriyaphap, T. Comparing Light—Emitting—Diodes light traps for catching anopheles mosquitoes in a forest setting, Western Thailand. *Insects* **2021**, *12*, 1076. [CrossRef]
13. Barrera, R. New tools for *Aedes* control: Mass trapping. *Curr. Opin. Insect Sci.* **2022**, *52*, 100942. [CrossRef] [PubMed]
14. Ong, J.; Chong, C.-S.; Yap, G.; Lee, C.; Abdul Razak, M.A.; Chiang, S.; Ng, L.-C. Gravitrap deployment for adult *Aedes aegypti* surveillance and its impact on dengue cases. *PLoS Negl. Trop. Dis.* **2020**, *14*, e0008528. [CrossRef]
15. Bertola, M.; Fornasiero, D.; Sgubin, S.; Mazzon, L.; Pombi, M.; Montarsi, F. Comparative efficacy of BG-Sentinel 2 and CDC-like mosquito traps for monitoring potential malaria vectors in Europe. *Parasites Vectors* **2022**, *15*, 160. [CrossRef] [PubMed]
16. Namango, I.H.; Marshall, C.; Saddler, A.; Ross, A.; Kaftan, D.; Tenywa, F.; Makungwa, N.; Odufuwa, O.G.; Ligema, G.; Ngonyani, H. The Centres for Disease Control light trap (CDC-LT) and the human decoy trap (HDT) compared to the human landing catch (HLC) for measuring *Anopheles* biting in rural Tanzania. *Malar. J.* **2022**, *21*, 181. [CrossRef] [PubMed]
17. Jaffal, A.; Fite, J.; Baldet, T.; Delaunay, P.; Jourdain, F.; Mora-Castillo, R.; Olive, M.-M.; Roiz, D. Current evidences of the efficacy of mosquito mass-trapping interventions to reduce *Aedes aegypti* and *Aedes albopictus* populations and *Aedes*-borne virus transmission. *PLoS Negl. Trop. Dis.* **2023**, *17*, e0011153. [CrossRef]
18. Pan, C.-Y.; Cheng, L.; Liu, W.-L.; Su, M.P.; Ho, H.-P.; Liao, C.-H.; Chang, J.-H.; Yang, Y.-C.; Hsu, C.-C.; Huang, J.-J. Comparison of fan-traps and gravitraps for aedes mosquito surveillance in Taiwan. *Front. Public Health* **2022**, *10*, 778736. [CrossRef]
19. Singapore Government. National Environment Agency. Available online: <https://www.nea.gov.sg/our-services/pest-control/fumigation> (accessed on 21 July 2024).
20. Park, M.-G.; Choi, J.; Hong, Y.-S.; Park, C.G.; Kim, B.-G.; Lee, S.-Y.; Lim, H.-J.; Mo, H.-h.; Lim, E.; Cha, W. Negative effect of methyl bromide fumigation work on the central nervous system. *PLoS ONE* **2020**, *15*, e0236694. [CrossRef]
21. Nelsen, J.A.; Yee, D.A. Mosquito larvicides disrupt behavior and survival rates of aquatic insect predators. *Hydrobiologia* **2022**, *849*, 4823–4835. [CrossRef]
22. Bravo, D.T.; Lima, G.A.; Alves, W.A.L.; Colombo, V.P.; Djogbenou, L.; Pamboukian, S.V.D.; Quaresma, C.C.; de Araujo, S.A. Automatic detection of potential mosquito breeding sites from aerial images acquired by unmanned aerial vehicles. *Comput. Environ. Urban Syst.* **2021**, *90*, 101692. [CrossRef]
23. Hanif, A.S.; Han, X.; Yu, S.-H. Independent control spraying system for UAV-based precise variable sprayer: A review. *Drones* **2022**, *6*, 383. [CrossRef]
24. Oğuz-Ekim, P. TDOA based localization and its application to the initialization of LiDAR based autonomous robots. *Robot. Auton. Syst.* **2020**, *131*, 103590. [CrossRef]
25. Nasir, F.E.; Tufail, M.; Haris, M.; Iqbal, J.; Khan, S.; Khan, M.T. Precision agricultural robotic sprayer with real-time Tobacco recognition and spraying system based on deep learning. *PLoS ONE* **2023**, *18*, e0283801. [CrossRef]
26. Sun, Q.; Chen, J.; Zhou, L.; Ding, S.; Han, S. A study on ice resistance prediction based on deep learning data generation method. *Ocean Eng.* **2024**, *301*, 117467. [CrossRef]
27. Preethi, P.; Mamatha, H.R. Region-based convolutional neural network for segmenting text in epigraphical images. *Artif. Intell. Appl.* **2023**, *1*, 119–127. [CrossRef]
28. Akande, T.O.; Alabi, O.O.; Ajagbe, S.A. A deep learning-based CAE approach for simulating 3D vehicle wheels under real-world conditions. *Artif. Intell. Appl.* **2022**, 1–11. [CrossRef]
29. Baltazar, A.R.; Santos, F.N.d.; Moreira, A.P.; Valente, A.; Cunha, J.B. Smarter robotic sprayer system for precision agriculture. *Electronics* **2021**, *10*, 2061. [CrossRef]

30. Wang, B.; Yan, Y.; Lan, Y.; Wang, M.; Bian, Z. Accurate detection and precision spraying of corn and weeds using the improved YOLOv5 model. *IEEE Access* **2023**, *11*, 29868–29882. [[CrossRef](#)]
31. Hu, C.; Xie, S.; Song, D.; Thomasson, J.A.; Hardin IV, R.G.; Bagavathiannan, M. Algorithm and system development for robotic micro-volume herbicide spray towards precision weed management. *IEEE Robot. Autom. Lett.* **2022**, *7*, 11633–11640.
32. Fan, X.; Chai, X.; Zhou, J.; Sun, T. Deep learning based weed detection and target spraying robot system at seedling stage of cotton field. *Comput. Electron. Agric.* **2023**, *214*, 108317.
33. Hassan, M.U.; Ullah, M.; Iqbal, J. Towards autonomy in agriculture: Design and prototyping of a robotic vehicle with seed selector. In Proceedings of the 2016 2nd International Conference on Robotics and Artificial Intelligence (ICRAI), Rawalpindi, Pakistan, 1–2 November 2016; pp. 37–44.
34. Zhang, C.; Lei, L.; Ma, X.; Zhou, R.; Shi, Z.; Guo, Z. Map Construction Based on LiDAR Vision Inertial Multi-Sensor Fusion. *World Electr. Veh. J.* **2021**, *12*, 261. [[CrossRef](#)]
35. Liu, Z.; Li, Z.; Liu, A.; Shao, K.; Guo, Q.; Wang, C. LVI-Fusion: A Robust Lidar-Visual-Inertial SLAM Scheme. *Remote Sens.* **2024**, *16*, 1524. [[CrossRef](#)]
36. Lee, J.; Hwang, S.; Kim, W.J.; Lee, S. SAM-Net: LiDAR depth inpainting for 3D static map generation. *IEEE Trans. Intell. Transp. Syst.* **2021**, *23*, 12213–12228. [[CrossRef](#)]
37. Shan, T.; Englot, B.; Meyers, D.; Wang, W.; Ratti, C.; Rus, D. Lio-sam: Tightly-coupled lidar inertial odometry via smoothing and mapping. In Proceedings of the 2020 IEEE/RSJ International Conference on Intelligent Robots and Systems (IROS), Las Vegas, NV, USA, 24 October 2020–24 January 2021; pp. 5135–5142.
38. Nourbakhsh, I.; Powers, R.; Birchfield, S. DERVISH an office-navigating robot. *AI Mag.* **1995**, *16*, 53.
39. Abiyev, R.H.; Günsel, I.; Akkaya, N.; Aytac, E.; Çağman, A.; Abizada, S. Robot soccer control using behaviour trees and fuzzy logic. *Procedia Comput. Sci.* **2016**, *102*, 477–484. [[CrossRef](#)]
40. Girshick, R. Fast r-cnn. In Proceedings of the 2015 IEEE International Conference on Computer Vision, Santiago, Chile, 7–13 December 2015; pp. 1440–1448.
41. Ren, S.; He, K.; Girshick, R.; Sun, J. Faster r-cnn: Towards real-time object detection with region proposal networks. *IEEE Trans. Patt. Anal. Mach. Intell.* **2016**, *39*, 1137–1149. [[CrossRef](#)] [[PubMed](#)]
42. Yan, J.; Lei, Z.; Wen, L.; Li, S.Z. The fastest deformable part model for object detection. In Proceedings of the IEEE Conference on Computer Vision and Pattern Recognition, Columbus, OH, USA, 23–28 June 2014; pp. 2497–2504.
43. Redmon, J.; Divvala, S.; Girshick, R.; Farhadi, A. You only look once: Unified, real-time object detection. In Proceedings of the IEEE Conference on Computer Vision and Pattern Recognition, Las Vegas, NV, USA, 27–30 June 2016; pp. 779–788.
44. Talaat, F.M.; ZainEldin, H. An improved fire detection approach based on YOLO-v8 for smart cities. *Neural. Comput. Appl.* **2023**, *35*, 20939–20954. [[CrossRef](#)]
45. What is YOLOv8? The Ultimate Guide. Available online: <https://blog.roboflow.com/whats-new-in-yolov8/#what-is-yolov8> (accessed on 10 July 2024).
46. Minakshi, M.; Bhuiyan, T.; Kariev, S.; Kaddumukasa, M.; Loum, D.; Stanley, N.B.; Chellappan, S.; Habomugisha, P.; Oguttu, D.W.; Jacob, B.G. High-accuracy detection of malaria mosquito habitats using drone-based multispectral imagery and Artificial Intelligence (AI) algorithms in an agro-village peri-urban pastureland intervention site (Akonyibedo) in Unyama SubCounty, Gulu District, Northern Uganda. *J. Public Health Epidemiol.* **2020**, *12*, 202–217.
47. Jeyabal, S.; Sachintha, W.; Bhagya, S.; Samarakoon, P.; Elara, M.R.; Sheu, B.J. Hard-to-Detect Obstacle Mapping by Fusing LIDAR and Depth Camera. *IEEE Sens. J.* **2024**, *24*, 24690–24698. [[CrossRef](#)]

**Disclaimer/Publisher’s Note:** The statements, opinions and data contained in all publications are solely those of the individual author(s) and contributor(s) and not of MDPI and/or the editor(s). MDPI and/or the editor(s) disclaim responsibility for any injury to people or property resulting from any ideas, methods, instructions or products referred to in the content.